Received: Added at production | Revised: Added at production | Accepted: Added at production

DOI: xxx/xxxx

ARTICLE TYPE

Thermo-mechanical modeling of the temperature dependent forming behavior of thermoplastic prepregs

Jean-Paul Ziegs*[1] | Daniel Weck[2] | Maik Gude[2] | Markus Kästner[1]

[1]Institute of Solid Mechanics, TU Dresden, Germany
[2]Institute of Lightweight Engineering and Polymer Technology, TU Dresden, Germany

Correspondence
*Jean-Paul Ziegs,
George-Bähr-Str. 3c, 01069 Dresden
Email: jean-paul.ziegs@tu-dresden.de

Funding Information
The project "Saxon Alliance for Material- and Resource-Efficient Technologies (AMARETO)" is funded by the European Union (European Regional Development Fund) and by the Free State of Saxony. Grant Number: 100291445

Abstract

Numerical optimization of the manufacturing process of hybrid lightweight structures consisting of fiber-reinforced plastics (FRP) is of high importance. It can reduce the time to market and can also avoid the production of costly prototypes. To model the considered thermoforming process, the temperature dependent deformation mechanisms have to be characterized and modeled within a finite element framework. An industry-oriented approach based on the parameterization of a material model implemented in LS-DYNA is introduced. The accordingly parameterized material model for the FRP is eventually applied in the simulation of thermoforming processes to show the influence of process and material parameters on the forming behavior of thermoplastic prepregs.

KEYWORDS:
thermoplastics, thermo-mechanical modeling, fiber-reinforced plastic, parameter identification, thermoforming

1 | INTRODUCTION

In recent years the popularity of lightweight components consisting of fiber-reinforced plastics (FRP) is steadily increasing in automotive and aerospace lightweight design due to its low density, good mechanical properties, energy efficiency and the possibility for recycling[1]. Besides some constraints the versatility of material combinations (matrix and fiber) ranging from short fiber mats to continuous fiber-reinforced composites as well as from randomly distributed fibers to laminates with defined fiber directions[1]. Also, the type of the semi-finished products can be distinguished in e.g. dry fabrics and pre-impregnated FRPs[1] called organo-sheets or prepregs. The advantage of the latter in the manufacturing process is that there is no need for an additional time-consuming consolidation process[2]. Due to this wide range of material, the development of the manufacturing process is often characterized by trial and error. In order to reduce the time to market and production expenses, simulations of the manufacturing processes are needed to determine optimal material and process parameter combinations. This paper is focused on the modeling of thermoforming processes using continuous biaxial-reinforced organo-sheets. Such materials are characterized by high tension, shear and bending resistance at room temperature and they become formable due to reduced shear and bending stiffnesses at temperatures above the melting point T_m while still having a high in-plane tensile stiffness. To model the complex deformation behavior in the full temperature range is very challenging. In the past complex material models are introduced to cover the temperature dependent deformation behavior of FRPs. JOHNSON[3] investigated the thermoforming process of fiber-reinforced thermoplastic sheets by modeling the rheological behavior of the sheets and determining suitable material parameters. Because of the natural inhomogeneous material structure of FRPs, modeling approaches on different length scales are used to predict the temperature dependent deformation behavior of composites. BAI[4] et.al. models the thermo-visco-plastic behavior

[0]**Abbreviations:** CF, carbon fibers; CLT, classical laminate theory; FRP, fiber-reinforced thermoplastic; PA6.6, polyamide 6.6; PFT, picture-frame test

on a micro scale, GUZMAN-MALDONADO[5] et.al. on a macro scale and MARON[6] describes the forming behavior using a multi-scale approach.
This paper presents an industry-oriented approach based on the parameterization of a macroscopic material model implemented in the finite element software LS-DYNA. Suited model parameters are determined by experimental testing and datasheets provided by the manufacturer. Numerical simulations of the thermoforming process allow to investigate the influence of process and material parameters.

2 | MODELING APPROACH AND CONSTITUTIVE EQUATIONS

During forming of a plane textile-reinforced polymer into a three-dimensional shape, three basic deformation mechanisms - shear, tension and bending - can be observed. Since the material behavior of the polymer matrix is strongly temperature dependent, a high influence of the temperature on the deformation behavior is observed. The temperature dependent deformation behavior of organo-sheets is modeled using the constitutive model MAT249_REINFORCED_THERMOPLASTIC provided by the FE-software LS-DYNA[7].
This material model assumes and additive decomposition of the total stress in the organo-sheet

$$\boldsymbol{\sigma}^{\mathrm{tot}} = \boldsymbol{\sigma}^{\mathrm{m}} + \boldsymbol{\sigma}^{\mathrm{f}} \tag{1}$$

into contributions of the matrix $\boldsymbol{\sigma}^{\mathrm{m}}$ and the fiber reinforcement $\boldsymbol{\sigma}^{\mathrm{f}}$. The first one is modeled by an hypoelastic-plastic constitutive law where the mechanical properties may be defined as functions of the temperature. Within the framework of hypoplasticity the constitutive equations are formulated in rate form

$$\overset{\Delta}{\boldsymbol{\sigma}}^{\mathrm{m}} = \mathbf{C}^{\mathrm{m}}\left[E^{\mathrm{m}}(T), \nu^{\mathrm{m}}(T)\right] : \mathbf{d}^{\mathrm{m}}_{\mathrm{el}} \tag{2}$$

where $\overset{\Delta}{\boldsymbol{\sigma}}^{\mathrm{m}}$ is the objective JAUMANN stress rate, $\mathbf{C}^{\mathrm{m}}$ the elasticity tensor which depends on the YOUNGs modulus E^{m} and the POISSON's ratio ν^{m}. The total rate of deformation

$$\mathbf{d}^{\mathrm{m}} = \mathbf{d}^{\mathrm{m}}_{\mathrm{el}} + \mathbf{d}^{\mathrm{m}}_{\mathrm{pl}} + \mathbf{d}^{\mathrm{m}}_{\mathrm{th}} \tag{3}$$

is composed in an elastic $\mathbf{d}^{\mathrm{m}}_{\mathrm{el}}$, plastic $\mathbf{d}^{\mathrm{m}}_{\mathrm{pl}}$ and thermal $\mathbf{d}^{\mathrm{m}}_{\mathrm{th}}$ part. An associative flow rule

$$\mathbf{d}^{\mathrm{m}}_{\mathrm{pl}} = \lambda^{\mathrm{m}}_{\mathrm{pl}} \frac{\partial \mathcal{F}}{\partial \boldsymbol{\sigma}^{\mathrm{m}}} \tag{4}$$

combined with the VON MISES yield criterion

$$\mathcal{F} = \frac{3}{2}\mathbf{s}^{\mathrm{m}} : \mathbf{s}^{\mathrm{m}} - \sigma_{\mathrm{y}}^{\mathrm{m}^2}\left(\bar{\varepsilon}^{\mathrm{m}}_{\mathrm{pl}}, T\right) \leq 0 \tag{5}$$

describes the evolution of plastic deformation. In eq. (4) and (5) $\lambda^{\mathrm{m}}_{\mathrm{pl}}$ is the plastic multiplier, $\mathbf{s}^{\mathrm{m}} = \boldsymbol{\sigma}^{\mathrm{m}} - \frac{1}{3}\mathbf{I}\,\mathrm{tr}\,\boldsymbol{\sigma}^{\mathrm{m}}$ the deviatoric part of the matrix stress and $\sigma_{\mathrm{y}}^{\mathrm{m}}\left(\bar{\varepsilon}^{\mathrm{m}}_{\mathrm{pl}}, T\right)$ the temperature dependent flow curve. The thermoforming simulations in Chapter 5 will be isothermal with varying process temperatures. As a consequence, the thermal expansion of the FRP can be neglected, $\mathbf{d}^{\mathrm{m}}_{\mathrm{th}} = 0$.
The fiber reinforcement is described by an anisotropic hyperelastic material law with up to three distinguished fiber directions. The tension/compression

$$\boldsymbol{\sigma}^{\mathrm{f}}_{\mathrm{Tension}} = \sum_{i=1}^{n} \frac{1}{J} f_i(\Lambda_i)(\mathbf{m}_i \otimes \mathbf{m_i}) \tag{6}$$

and shear

$$\boldsymbol{\sigma}^{\mathrm{f}}_{\mathrm{Shear}} = \sum_{i=1}^{2} \frac{1}{J} g_{i,i+1}(\gamma_{i,i+1})(\mathbf{m}_i \otimes \mathbf{m_{i+1}}) \tag{7}$$

behavior are decoupled and mainly defined by the relation between fiber stress and elongation $f_i(\Lambda_i)$ and shear response as a function of shear angles between the fibers $g_{i,i+1}(\gamma_{i,i+1})$. The deformation gradient $\mathbf{F}$ is used to calculate the JACOBIAN determinant $J = \det \mathbf{F}$ and to update the fiber orientation vector

$$\mathbf{m}_i = \mathbf{F} \cdot \mathbf{m}^0_i \tag{8}$$

of the i-th fiber family depending on their initial orientation $\mathbf{m}^0_i$. With the current fiber direction the stretch of each fiber

$$\Lambda_i = |\mathbf{m}_i| \tag{9}$$

and the shear angle between two fiber families

$$\cos(\gamma_{i,i+1}) = \frac{\mathbf{m}_i \cdot \mathbf{m}_{i+1}}{|\mathbf{m}_i| \cdot |\mathbf{m}_{i+1}|} \tag{10}$$

are calculated respectively.

The different deformation behavior of organo-sheets in the wide temperature range is mostly affected by the varying stiffness of the matrix material. In order to model a stiff composite at room temperature which becomes deformable with increasing temperatures, a layer wise modeling approach of the FRP is used, Fig. 1. Each layer contains either the matrix part or the fiber part of the material model (1) by setting the parameters of the other constitutive equations to zero. In the reinforcement layer two fiber families oriented perpendicular to each other within the plane are included. Due to this modeling approach the height of the matrix h^{m} and fiber h^{f} layers will enter the parameter set as volume fractions of either the matrix $\varphi^{\mathrm{m}} = \frac{h^{\mathrm{m}}}{h}$ or the fiber $\varphi^{\mathrm{f}} = \frac{h^{\mathrm{f}}}{h}$ distribution by dividing them with the total height h. The here called volume fractions of the matrix and fiber contributions are not that ones which can be physically measured but those which are required in the finite element model to predict the effective in-plane tension and shear as well as the out-of-plane bending behavior accurately.

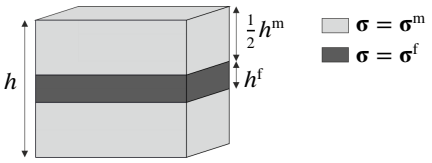

FIGURE 1 Layer wise modeling approach of the FRP.

3 | MATERIAL CHARACTERIZATION

In this paper the deformation behavior of pre-consolidated composites, so called organo-sheets with a polyamide 6.6 (PA6.6) thermoplastic matrix and carbon fibers (CF) as reinforcement, is investigated. The organo-sheets were made by consolidating biaxial reinforced weft-knitted fabrics. This section explains the acquisition of the material data which is needed in order to determine the model parameters for the constitutive laws introduced in the previous chapter. The required parameters are summarized in table 1. Temperature dependent material data must be determined from room temperature T_{r} up to the process temperature T_{p} which has to be above the melting point T_{m} of the polymer matrix. The procedure can be divided into two approaches. The first one is data extraction of the data sheet for PA6.6 provided by the manufacturer BASF. In addition, different experiments are performed to characterize the temperature dependent material behavior of the composite.

TABLE 1 Required model parameter.

Matrix		**Reinforcement**	
Parameter	**Sign**	**Parameter**	**Sign**
Temperature dependent matrix stiffness	$E^{\mathrm{m}}(T)$	Fiber stress as function of fiber strain	$f_i(\Lambda_i)$
Temperature dependent POISSON's ratio	$\nu^{\mathrm{m}}(T)$	Shear stress as function of shear angle	$g_{i,i+1}(\gamma_{i,i+1})$
Temperature dependent flow rules	$\sigma_{\mathrm{y}}^{\mathrm{m}}(\bar{\varepsilon}_{\mathrm{pl}}^{\mathrm{m}}, T)$		
Volume fraction of matrix	φ^{m}	Volume fraction of reinforcement	φ^{f}

3.1 | BASF data sheet for Polyamide 6.6

From the data sheet[8] of a PA6.6 namely Ultramid®A3K - PA66 provided by the manufacturer BASF, information about this thermoplastic polymer can be gathered. For the purpose of finding the required model parameters for the matrix constitutive equations (2) - (5) the tensile stress-strain curves at varying temperatures, the glass transition temperature $T_g = 72\,°C$ and melting point $T_m = 260\,°C$ are used. The stress-strain curves are given in a temperature range from $-40\,°C$ to $150\,°C$ and depicted in Figure 2(a). Based on these curves the temperature dependent stiffnesses of the polymer matrix $E^m(T)$ Fig. 2(b) are determined using the tangent modulus between $\varepsilon = 0.05\,\%$ and $\varepsilon = 0.25\,\%$ as suggested by EHRENSTEIN[9]. Reference[9] also provides an opportunity to determine the flow curves $\sigma_y^m\left(\bar{\varepsilon}_{pl}^m, T\right)$ Fig. 2(c) which describe the plastic behavior of the matrix material. In order to form the prepreg, the process temperature T_p needs to be above the melting point $T_p > T_m$. For this reason an extrapolation of $E^m(T)$ and $\sigma_y^m\left(\bar{\varepsilon}_{pl}^m, T\right)$ to about $280\,°C$ which is required for the desired simulation of the thermoforming process is presented in Chapter 4.

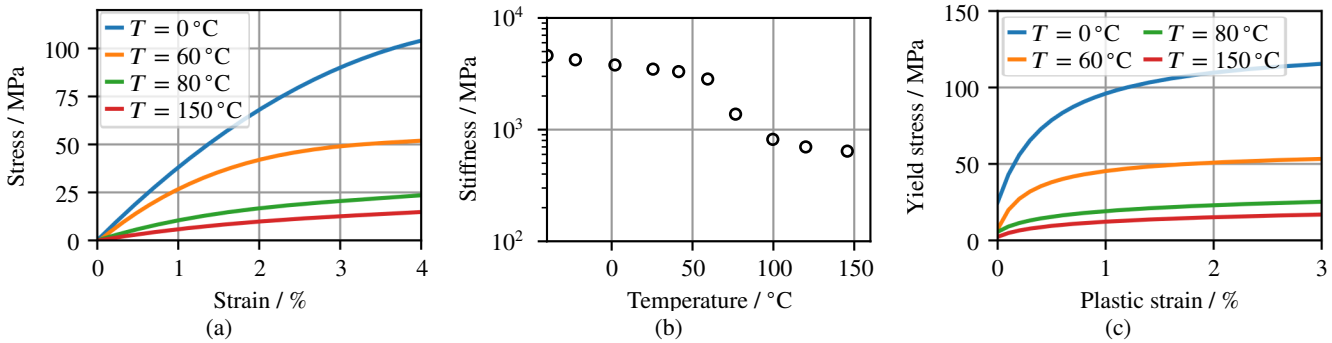

FIGURE 2 Extracted data for temperature dependent stress vs. strain curves for Polyamide 6.6 in the temperature range from $-40\,°C$ to $150\,°C$ provided by BASF[8] (a), and determined Stiffnesses (b) and Flow curves (c) by the approach of EHRENSTEIN[9].

3.2 | Experimental data

To characterize the temperature deformation behavior of prepregs, three different tests are performed. Regarding the intended simulation of the thermoforming process, the parameter identification around process temperature $T_p \approx 280\,°C$ is focused. The gathered experimental data are the force-displacement curves under tensile loads, the temperature dependent bending stiffness and shear force as a function of the shear angle. The characteristic behavior for in-plane tension is determined from tensile tests on strip specimens following DIN EN ISO 13934-1[10] Fig. 3(a). The recorded force-displacement curves of the performed test at $150\,°C$, loaded separately in each fiber direction are shown in Figure 4(a). The low test temperature was decided due to clamping issues of the prepreg strip if the thermoplastic matrix becomes too soft. Because of the tensile behavior of FRPs loaded in fiber direction depends just slightly on the temperature[6] and tension is not a main deformation mode of the here considered composites[6] , the received data is assumed to be meaningful enough to model the manufacturing process. Gravimetric cantilever tests according to DIN 53362[11], Fig. 3(b), may be used to determine the temperature dependent bending stiffness of the organo-sheet, Fig. 4(b). The test procedure was based on HARRISON[12] et. al. The typically non-linear shear force vs. shear angle curves, Fig. 4(c) are recorded using the picture-frame test (PFT) at a process temperature of $T_p = 280\,°C$, Figure 3(c), as described by HARISSON[13] et. al. In addition, experimental data at room temperature of the same test of an unconsolidated biaxial weft-knitted fabric, similar to that used for manufacturing the organo-sheets are provided by the Institute of Textile Machinery and High Performance Material Technology (ITM). Later, this information will be helpful to identify the shear behavior of the textile contribution $g_{i,i+1}(\gamma_{i,i+1})$. Furthermore, the dimensions and weight of some consolidated FRP samples are conventionally measured to determine the height h and the density ρ of the composite.

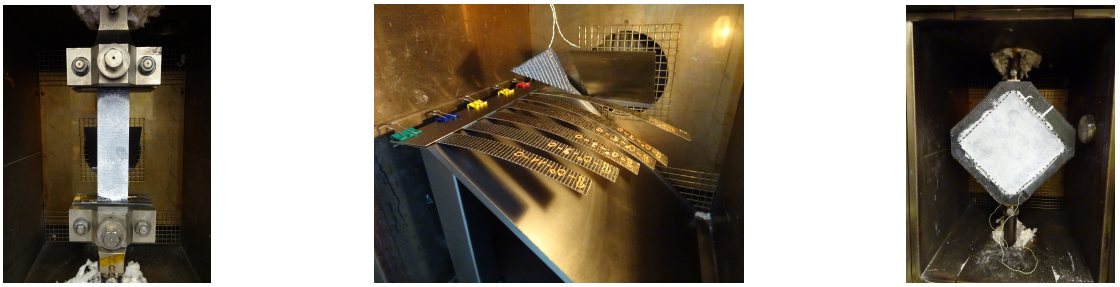

(a) (b) (c)

FIGURE 3 Experimental setup of the tension (a), cantilever (b) and picture-frame test (c).

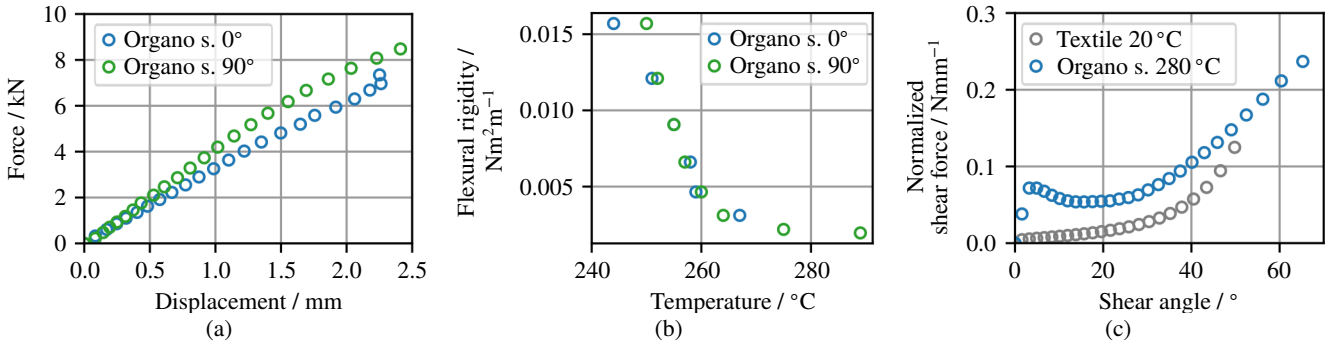

FIGURE 4 Experimental data for: (a) tension test of the prepreg at 150 °C , (b) bending behavior of the prepreg from 240 °C - 300 °C and (c) shear deformation of a biaxial reinforced weft knitted fabric at room temperature and the prepreg at 280 °C.

4 | MODEL PARAMETER IDENTIFICATION

Following section describes a method to determine the required model parameters for the constitutive equations provided in Chapter 2 with the help of the acquired material data presented in Section 3. At first the temperature dependent stiffness $E^{\mathrm{m}}(T)$ and yield behavior $\sigma_{\mathrm{y}}^{\mathrm{m}}(\bar{\varepsilon}_{\mathrm{pl}}^{\mathrm{m}}, T)$ of the polymer matrix need to be extrapolated to model the behavior at higher temperatures. Due to an additional phase change of the thermoplastic from solid to fluid only an extrapolation close to the melting point $T < T_{\mathrm{m}}$ is presented at this point. An ARRHENIUS type equation is used to find a relation of the stiffness and the temperature below the glass transition temperature T_{g}, Fig. 5(a) blue solid line. In order to fit the data points above T_{g} as well as extrapolate the matrix stiffness to higher temperatures, a WILHELM-LANDEL-FERRY relation is used as shown in Figure 5(a), orange solid line. A common approach to extrapolate yield curves for higher effective plastic strains is the well-known GOSH-ansatz

$$\sigma_{\mathrm{y}}^{\mathrm{m}}\left(\bar{\varepsilon}_{\mathrm{pl}}^{\mathrm{m}}, T\right) = b(T) \cdot \left(c(T) + \bar{\varepsilon}_{\mathrm{pl}}^{\mathrm{m}}\right)^{n(T)} + e(T) \tag{11}$$

that was also used for the mathematical description of the flow curve of thermoplastics by BEHRENS [14] et.al. By finding a relation between the coefficients $b(T)$, $c(T)$, $n(T)$ and $e(T)$, equation (11) is also suitable to identify the yield behavior of the thermoplastic at higher temperatures below the melting point $T < T_{\mathrm{m}}$. These temperature dependent functions are evaluated using flow curves from Figure 2(c). Some examples for such extrapolated flow curves are depicted in Figure 5(b). From the experimental data of the tension test Fig. 4(a), the effective tensile behavior of the prepreg can be characterized. A constant effective stiffness of the composite is suited to model the observed linear tensile behavior of the FRP. Consequently the functions $g_i(\Lambda_i)$ which describes the fiber stress as a function of stretch, reduce to two constant elastic moduli $f_i(\Lambda_i) = E_{\alpha}^{\mathrm{f}}$. The number $i = 1, 2$ of the fiber families is substituted by α which corresponds to the direction of the fiber families $i = 1 \rightarrow \alpha = 0\,°$ or $i = 2 \rightarrow \alpha = 90\,°$. Using the rule of mixture

$$E_{\alpha}^{\mathrm{eff}}(T) = \varphi^{\mathrm{f}} E_{\alpha}^{\mathrm{f}} + \left(1 - \varphi^{\mathrm{f}}\right) E^{\mathrm{m}}(T) \tag{12}$$

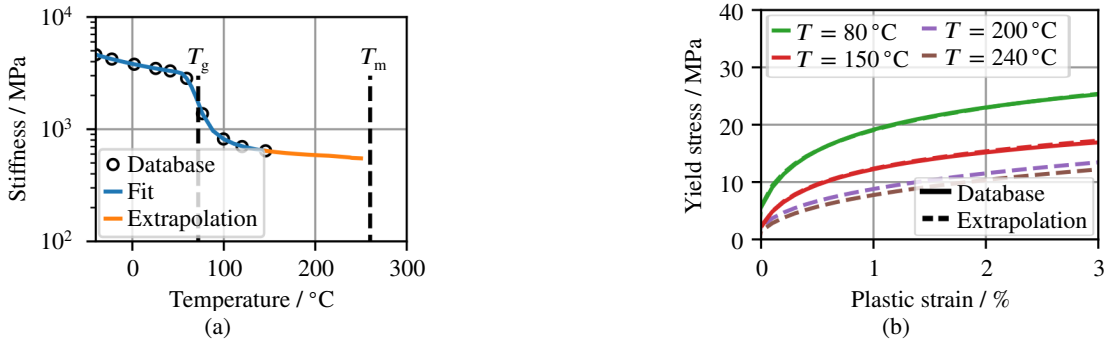

FIGURE 5 Extrapolated temperature dependent stiffness (a) and flow curves (b) up to 240 °C of Polyamide 6.6 matrix.

and knowing the matrix and effective stiffness of the FRP at $T = 150\,°C$ from Figures 5(a) and 4(a) the products $E_\alpha^f \varphi^f$ (for $\alpha = 0\,°/90\,°$) can be determined. Introducing the classical laminate theory (CLT) the bending stiffness

$$B_\alpha(T) = f\left(E^m(T), E_\alpha^f, \varphi^f\right) \tag{13}$$

of the composite can be determined using the in-plane stiffnesses and volume fractions as described by SCHÜRMANN [15]. Using the extrapolated matrix stiffness Fig. 5(a) and the experimental results of the bending test Fig. 4(b), equation (13) is evaluated for $T = 250\,°C$ and provides another relation for E_α^f and φ^f. The results for $E_\alpha^{eff}(T = 150\,°C)$ by equation (12) and $B_\alpha(T = 250\,°C)$ using equation (13) enable the determination of the volume fractions φ^f, φ^m and the fiber stiffnesses E_α^f. Furthermore, the matrix stiffness $E^m(T)$ can now be calculated invertible by fitting the experimental data shown in Figure 4(b) and the numerical results of the flexural rigidity. Figures 6 (b) and (c) show the comparison of the bending stiffnesses in the relevant temperature range between experimental, simulated and theoretical data using the CLT. Slightly differences between CLT and finite element results occur due to a trapezoidal integration scheme in the thickness direction in LS-DYNA [16]. Because of the isotropic constitutive law of the matrix material and the fact $\varphi^f << \varphi^m$ the simulated results will result only in negligible differences when bending the organo-sheet by the 0 ° or 90 ° direction according to the experimental observations in Figure 4(b). Next step will be the modeling

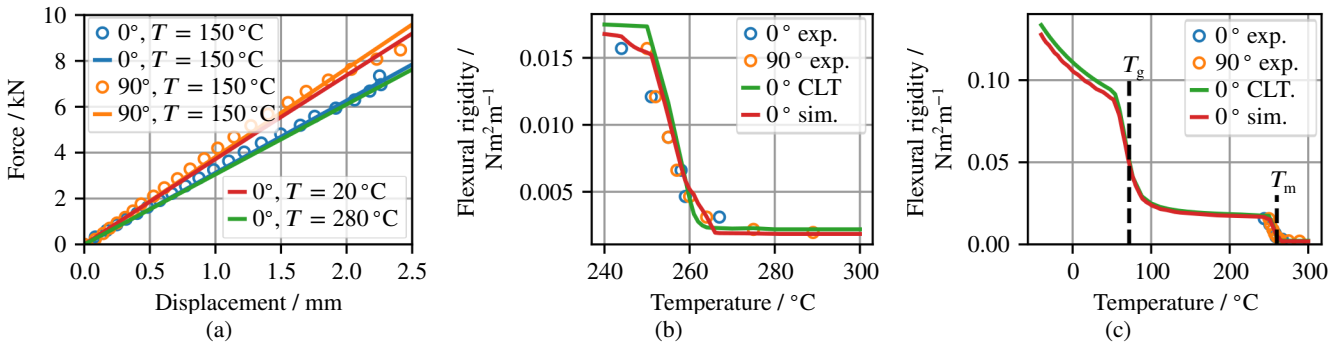

FIGURE 6 (a) Comparison of force vs. displacement curve of the experimental (circles) and simulated (solid lines) tensile test of the organo-sheet at 150 °C. (b) Modelled temperature dependent bending stiffness of the organo-sheet around the melting temperature and (c) in the whole temperature range compared with analytical values by classical laminate theory.

of the shear deformation behavior of the pre-consolidated FRP accordingly to the experimental results showing in Figure 4(c). In the beginning the material shows a significantly higher shear resistance until reaching a peak. Subsequently, the shear stiffness becomes very low and increases distinctly after a shear angle of about 30°. The stiff response at the start is caused by the PA6.6 matrix. Assuming ideal plasticity of the polymer when reaching the melting temperature T_m prevents a further strong increase of the composite's shear stiffness. Another increase of the shear modulus can still be attained via the fiber contribution. By looking at the shear force vs. shear angle curve of the unconsolidated fabric in Figure 4(c) a low shear resistance at small angles which rises at higher ones can be observed. Besides an offset this behavior matches the shear behavior of the organo-sheet after the

peak force. Identifying the stress threshold of the matrix' ideal plasticity and modeling the shear behavior of the dry fabric will lead to the shear deformation characteristic of the consolidated composite when combining both. One opportunity offered by LS-DYNA with the chosen material model MAT249 is to calculate the shear behavior of the reinforcement

$$g_{i,i+1}(\gamma_{i,i+1}) = \begin{cases} G_{\text{low}} & \text{for} \quad \gamma_{i,i+1} \leq \gamma_{\text{crit}} \\ G_{\text{high}} & \text{else} \end{cases} \tag{14}$$

by a three-parameter model[7] (14). This approach uses one shear modulus below a so called critical or locking shear angle γ_{crit} and another one above this angle. In the sense of fabrics, the fibers cannot shear freely anymore above γ_{crit}, wrinkles will occur, and the shear resistance increases. In order to determine the shear moduli and the critical shear angle for the three-parameter model experimental results of the unconsolidated textile at $T = 20\,°\text{C}$ provided by the ITM is used, Fig. 7(a). Combining the three-parameter model for the reinforcement contribution and the assumed ideal plasticity of the matrix allows to identify the yield stress of the polymer above the melting temperature T_{m} by fitting the experimental and numerical shear behavior shown in Figure 7(b). This approach is able to model the strong dependence of the shear resistance with respect to the forming temperature as depicted in Figure 7(c) and experimentally proven by HARRISON[13] and KLÖPPEL[17]. As a part of fitting the experimental

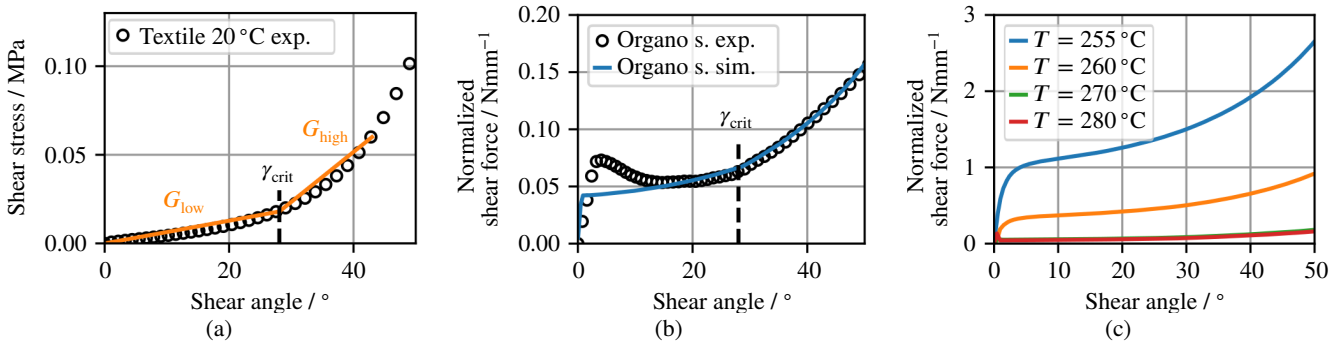

FIGURE 7 (a) Measured shear stress as a function of shear angle of the not consolidated biaxial weft-knitted fabric and linear regression to predict the shear stiffnesses below and above the critical shear angle. (b) Comparison of the experimental and numerically determined shear forces of the organo-sheet at $T = 280\,°\text{C}$. (c) Results of the picture frame test simulations at different temperatures.

observed bending and shear behavior of the prepreg, the mechanical properties, stiffness and yield behavior of the thermoplastic matrix above the melting temperature T_{m} could be determined as well. The so far missing POISSON's ratio of the polymer is assumed to be constant while in the solid state and set to $\nu^{\text{m}}(T < T_{\text{m}}) = 0.4$ as an often used value for PA6.6[9,1]. As soon as the matrix will change into its molten phase it is assumed to be incompressible which can be modeled by setting the POISSON's ratio to $\nu^{\text{m}}(T \geq T_{\text{m}}) = 0.499 \approx 0.5$. The results of the temperature depending properties of the thermoplastic matrix in the full temperature range are depicted in Figures 8(a) - (c). The presented and calibrated material model is able to predict the key deformation modes of prepregs and can be used to model their complex temperature dependent forming behavior which is necessary for the simulation of the thermoforming process of pre-impregnated thermoplastic composites.

5 | THERMOFORMING SIMULATION

The material model introduced and parameterized in the previous sections is used to investigate numerically the influence of the process temperature T_{p} and initial fiber orientation m_i^0 while forming the organo-sheet. Figure 9(a) shows the considered T-shape geometry. The highlighted concave area is a very critical region which is hard to enclose/attach by the composite. For this reason, all the examinations provided in this section will refer to this area. According to MARON[6], forming of prepregs is mainly enabled by shear and bending deformation. While forming, a theoretical fiber alignment in the considered area will be developed depending on the initial fiber orientation as shown in Figure 9(b,c). During manufacturing, the material needs to be formed onto the concave curved flange in the highlighted area. If the circumferential direction of the flange is between the fibers, as granted by an initial orientation of $m_i^0 = 0\,°/90\,°$, shear deformation is possible. Evidence is provided by the simulation of the

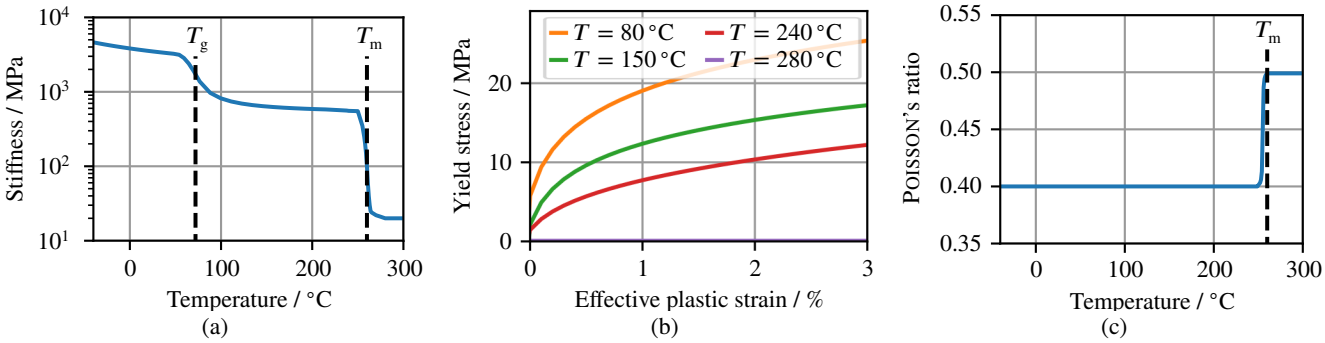

FIGURE 8 Modelled temperature dependent stiffness (a), flow curves around the melting temperature (b) and POISSON's ratio as described in the beginning of this section of the PA6.6. matrix.

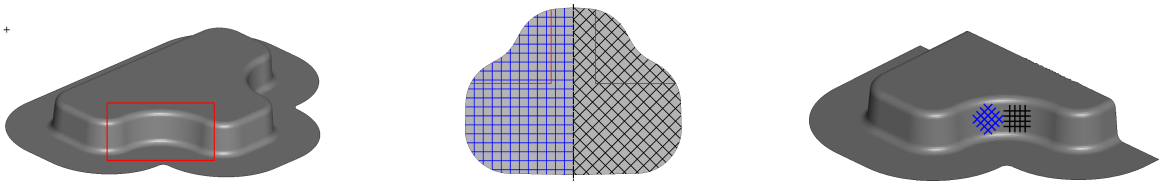

FIGURE 9 (a) Punch geometry for thermoforming process and highlighted investigated part. (b) Considered initial fiber orientations and (c) ideal assumed fiber directions while forming at the investigated area.

manufacturing process, Fig. 10, at the same process temperature $T_p = 280\,°C$ and two different initial fiber orientations. In the concave area higher shear angles will be reached in the case of $m_i^0 = 0\,°/90\,°$, Fig. 10(a). If $m_i^0 = \pm 45\,°$ shear deformation in this region is almost impossible which will cause the occurrence of defects like wrinkles shown in Figure 10(b). Another important

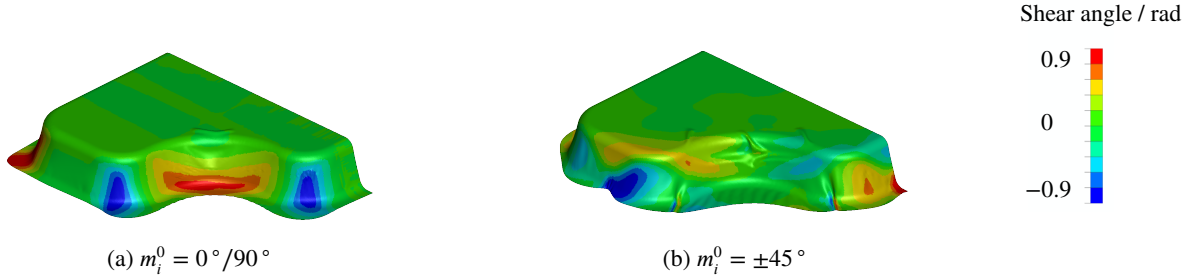

FIGURE 10 Comparison of shear angles and formed shapes of the draped thermoplastic prepreg at $T_p = 280\,°C$ for different initial fiber orientations.

phenomenon that is to be considered in the development of the manufacturing process is the material feeding influenced by m_i^0. Figure 11 shows the material contour of the undeformed and deformed composite with respect to the initial fiber orientation. Obviously, the material flow in the case of $m_i^0 = 0\,°/90\,°$ is more likely to the aimed shape. As a consequence, manufacturing simulations are a useful method for the optimization of the blank shapes and able to support the reduction of material waste. Another investigation refers to the influence of the process temperature T_p. Figure 12 shows the shear angle distribution on the formed composites for an initial fiber orientation $m_i^0 = 0\,°/90\,°$ for decreasing process temperatures T_p. With lower T_p, the matrix stiffness and so the shear resistance of the composite increases. Consequently, lower shear angles occur during the manufacturing process, the material extension becomes less and this will cause the shape of the manufactured part not to be of

(a) $m_i^0 = 0\,°/90\,°$ (b) $m_i^0 = \pm 45\,°$

FIGURE 11 Material feeding visualized by composite contour before (dashed line) and after (solid line) manufacturing with different initial fiber orientation.

high quality. With the numerical treatment of the thermoforming process the investigation of more manufacturing parameters

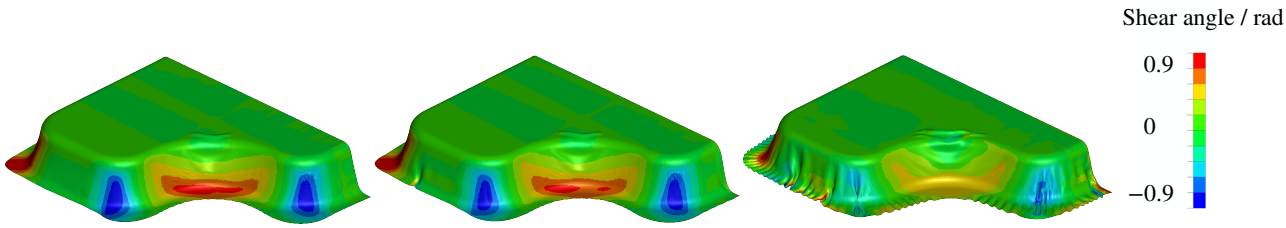

(a) $T_\mathrm{p} = 280\,°\mathrm{C}$ (b) $T_\mathrm{p} = 260\,°\mathrm{C}$ (c) $T_\mathrm{p} = 250\,°\mathrm{C}$

FIGURE 12 Shear angle distribution of formed composite for $m_i^0 = 0\,°/90\,°$ for different forming temperatures.

like binder forces or friction coefficients is possible. This makes simulations well-suited for the determination of valid process and material parameter ranges in order to reduce the time consuming and expensive development of manufacturing processes.

6 | CONCLUSIONS

Lightweight composite components pose high demands on the development of the complex manufacturing process. In this context, simulative approaches play a supporting role in the identification of suitable process and material parameter combinations. This paper presents the simulation of the thermoforming process by using a pre-implemented material model provided in the FE-tool LS-DYNA. A method to determine the required temperature depending model parameters for the constitutive model by using literature and experimental data is described. The material behavior at various temperatures is numerically examined. Finally, the influence of the initial fiber direction and process temperature while thermofoming is investigated on a T-shaped geometry.

The simulation-assisted development of manufacturing processes is well-suited to identify optimal material and process parameter combinations. Future thermo-mechanical transient simulations may grant the prediction of the temperature distribution of the composite while thermoforming processes using variotherm tools and determine further advantageous process parameters.

ACKNOWLEDGMENTS

The authors acknowledge the support of the project “Saxon Alliance for Material- and Resource-Efficient Technologies (AMARETO)” (Project No 100291445) that is funded by the European Union (European Regional Development Fund) and by the Free State of Saxony.

Furthermore the authors appreciate the Institute of Textile Machinery and High Performance Material Technology (ITM) for providing the biaxial weft-knitted-fabrics as well as the Institute of Lightweight Engineering and Polymer Technology (ILK) for the manufacturing of the pre-consolidated composites and the support of the testing procedure.

The authors are grateful to the Centre for Information Services and High Performance Computing [Zentrum für Informationsdienste und Hochleistungsrechnen (ZIH)] TU Dresden for providing its facilities for high throughput calculations.

References

1. Schürmann H. *Konstruieren mit Faser-Kunststoff-Verbunden*. 2. Berlin Heidelberg: Springer . 2007.
2. Behrens BA, Raatz A, Hübner S, et al. Automated Stamp Forming of Continuous Fiber Reinforced Thermoplastics for Complex Shell Geometries. In: Procedia CIRP 66. ; 2017: 113-118.
3. Johnson A. Rheological model for the forming of fabric-reinforced thermoplastic sheets. *Composites Manufacturing* 1995; 6: 153-160.
4. Bai X, Bessa MA, Melro AR, Camanho PP, Guo L, Liu WK. High-fidelity micro-scale modeling of the thermo-visco-plastic behavior of carbon fiber polymer matrix composites. *Composite Structures* 2015; 134: 132-141.
5. Guzman-Maldonado E, Hamila N, Boisse P, Bikard J. Thermomechanical analysis, modelling and simulation of the forming of pre-impregnated thermoplastics composites. *Composites: Part A* 2015; 78: 211-222.
6. Maron B. *Beitrag zur Modellierung und Simulation des Thermoformprozesses von textilverstärkten Thermoplastverbunden*. Phd thesis. TU Dresden, 2015.
7. LST . *LS-DYNA Keyword User's Manual - Volume II Material Models*. r12 ed. 2020.
8. BASF . Datasheet: Ultramid®A3K - PA66. 2017. https://www.campusplastics.com/material/pdf/131807/UltramidA3K?sLg=en, CAMPUSPLASTICS Database. Accessed November 13, 2018.
9. Ehrenstein GW. *Mit Kunststoffen konstruieren: eine Einführung ; mit 33 Tabellen*. 2. Hanser . 2002.
10. DIN EN ISO 13934-1: Textilien – Zugeigenschaften von textilen Flächengebilden – Teil 1: Bestimmung der Höchstzugkraft und Höchstzugkraft-Dehnung mit dem Streifen-Zugversuch. 2013.
11. DIN 53362:2003-10 - Bestimmung der Biegesteifigkeit. 2003.
12. Harrison P, Alvarez MF, Correia N, Mimoso P, Cristovão C, Gomes R. Characterising the Forming Mechanics of Pre-Consolidated Nylon-Carbon Composite. In: 18th European Conference on Composite Materials. ; June 24–28, 2018; Athens.
13. Harrison P, Clifford M, Long A. Shear characterisation of viscous woven textile composites: a comparison between picture frame and bias extension experiments. *Composites Science and Technology* 2004; 64: 1453-1465.
14. Behrens BA, Vucetic M, Neumann A, Osiecki T, N.Grbic . Experimental test and FEA of a sheet metal forming process of composite material and steel foil in sandwich design using LS-DYNA. *Key Engineering Materials* 2015; 651-653: 439-445.
15. Schürmann H. *Konstruieren mit Faser-Kunststoff-Verbunden*. 2. ch. Klassische Laminattheorie des MSV als Scheiben- und Plattenelement: 323-340; Berlin Heidelberg: Springer . 2007.
16. LST . *LS-DYNA Keyword User's Manual - Volume I*. r12 ed. 2020.
17. Klöppel T, Knust G, Haufe A. New Developments to Capture the Manufacturing Process of Composite Structures in LS-DYNA. In: 12th LS-DYNA Developer Forum. ; 2013; Filderstadt.